© 2019. Published by The Company of Biologists Ltd | Development (2019) 146, dev167841. doi:10.1242/dev.167841

RESEARCH REPORT

TOP1α regulates *FLOWERING LOCUS C* expression by coupling histone modification and transcription machinery

Peiqiao Zhong, Jiaojiao Li, Linjie Luo, Zhong Zhao* and Zhaoxia Tian*

ABSTRACT

The key steps of transcription are coupled with the opening of the DNA helical structure and establishment of active chromatin to facilitate the movement of the transcription machinery. Type I topoisomerases cleave one DNA strand and relax the supercoiled structure of transcribed templates. How topoisomerase-mediated DNA topological changes promote transcription and establish a permissive histone modification for transcription elongation is largely unknown. Here, we show that TOPOISOMERASE 1α in plants regulates *FLOWERING LOCUS C* transcription by coupling histone modification and transcription machinery. We demonstrate that TOP1α directly interacts with the methyltransferase SDG8 to establish high levels of H3K36 methylation downstream of *FLC* transcription start sites and recruits RNA polymerase II to facilitate transcription elongation. Our results provide a mechanistic framework for TOP1α control of the main steps of early transcription and demonstrate how topoisomerases couple RNA polymerase II and permissive histone modifications to initiate transcription elongation.

KEY WORDS: Topoisomerase I, *FLOWERING LOCUS C*, H3K36 methyltransferase, RNA polymerase II, Transcription elongation, *Arabidopsis*

INTRODUCTION

Chromatin structure is a crucial determinant in the regulation of DNA replication and transcription. Opening the DNA helical structure in highly compact chromatin to recruit the transcription initiation complex and establishing the active chromatin state are two main steps of RNA polymerase II (RNAPII)-mediated transcription in all living cells. Topoisomerase 1 (TOP1) catalyzes the transient cleavages of one strand of DNA and participates in the relaxation of the supercoiled structure of transcription templates (Champoux, 2001). In plants, *TOPOISOMERASE 1α* (*TOP1α*), which encodes a type IB topoisomerase, was first isolated in *Arabidopsis thaliana* by its homology with yeast and human TOP1, and its ability to complement the phenotype of yeast *top1* mutants (Kieber et al., 1992). Mutations in this gene were later found to exhibit varied defects in several aspects of plant development, including primordia initiation and phyllotaxis (Laufs et al., 1998; Takahashi et al., 2002), and stem cell homeostasis in the shoot and floral meristems (Graf et al., 2010; Liu et al., 2014). Recently, *TOP1α* has been shown to play an important role in controlling flowering time by the direct activation of *FLOWERING LOCUS C* (*FLC*) and its homologs (Gong et al., 2017). It has been widely proved that histone methylations, such as H3K4me3 (He et al., 2004; Pien et al., 2008; Shafiq et al., 2014; Tamada et al., 2009) and H3K36me3 (Kim et al., 2005; Xu et al., 2008; Zhao et al., 2005), are required for generating the permissive chromatin state to maintain high-level transcriptions of *FLC*. However, how *TOP1α* modulates DNA topology to activate transcription and establish a permissive histone modification facilitating *FLC* transcription is largely unknown. Here, we show that TOP1α directly binds the H3K36me methyltransferase SET DOMAIN GROUP 8 (SDG8) and recruits RNAPII to facilitate *FLC* transcription elongation. Accordingly, in *top1α* and *sdg8* mutants, transcripts of *FLC* were dramatically decreased in the early stages of transcription elongation. Our study reveals that TOP1α, together with the H3K36me methyltransferase and RNAPII, controls the main steps of early transcription of *FLC*.

RESULTS AND DISCUSSION

H3K36 methylation levels at the *FLC* locus are reduced in *top1α* mutants

The *top1α* mutant exhibits an early flowering phenotype in both long-day and short-day conditions by directly repressing the expression of *FLC* (Fig. S1) (Gong et al., 2017). Moreover, *FLC* showed significant epistasis effects in the *top1α* mutant, in which early flowering phenotypes were completely suppressed by the overexpression of *FLC* (Gong et al., 2017). To genetically test the interaction between *FLC* and *TOP1α*, we crossed the *top1α-1* mutant (hereafter *top1α*) with *flc-3* in the Col background and observed that the *top1α flc-3* double mutant shows early flowering phenotypes similar to *top1α* or *flc-3* single mutants based on mean total rosette leaf number or flowering time (Fig. 1A,B). To confirm this observation, we also analyzed the flowering phenotypes of the *top1α flc-3* double mutant in the *FRIGIDA* (*FRI*) background, which contains high levels of *FLC* expression at the vegetative stage (Johanson et al., 2000; Michaels and Amasino, 2001). The *top1α* or *flc-3* single mutants in the *FRI* background flowered significantly earlier than wild-type *FRI* plants (Fig. 1A,B). Likewise, we also observed the same early flowering phenotypes in *top1α flc-3* double mutants in the *FRI* background (Fig. 1A,B). In agreement with these observations, *FLC* expression levels were observed to be downregulated in 8-day-old seedlings of these three mutants in both backgrounds (Fig. 1C,D).

FLC transcripts are more abundant in young tissues of shoot tips (Michaels and Amasino, 1999; Sheldon et al., 2002; Sung and Amasino, 2004). To test whether TOP1α proteins are colocalized with *FLC* transcripts in *Arabidopsis*, we transformed the *TOP1α::TOP1α-GFP* plasmid into *top1α* mutants and observed the full complementation of *top1α* early flowering phenotypes (Fig. S2). As predicted, we observed that both the mRNA and protein of *TOP1α* mainly accumulated in the shoot apical meristem and young leaves (Fig. S3), which was similar to *FLC*.

CAS Center for Excellence in Molecular Plant Sciences, School of Life Sciences, University of Science and Technology of China, Huangshan Road 443, Hefei 230027, China.

*Authors for correspondence (zhzhao@ustc.edu.cn; zxtian@ustc.edu.cn)

Z.Z., 0000-0001-8044-0409; Z.T., 0000-0002-6707-3576

Received 13 May 2018; Accepted 22 January 2019

Development (2019) 146, dev167841. doi:10.1242/dev.167841

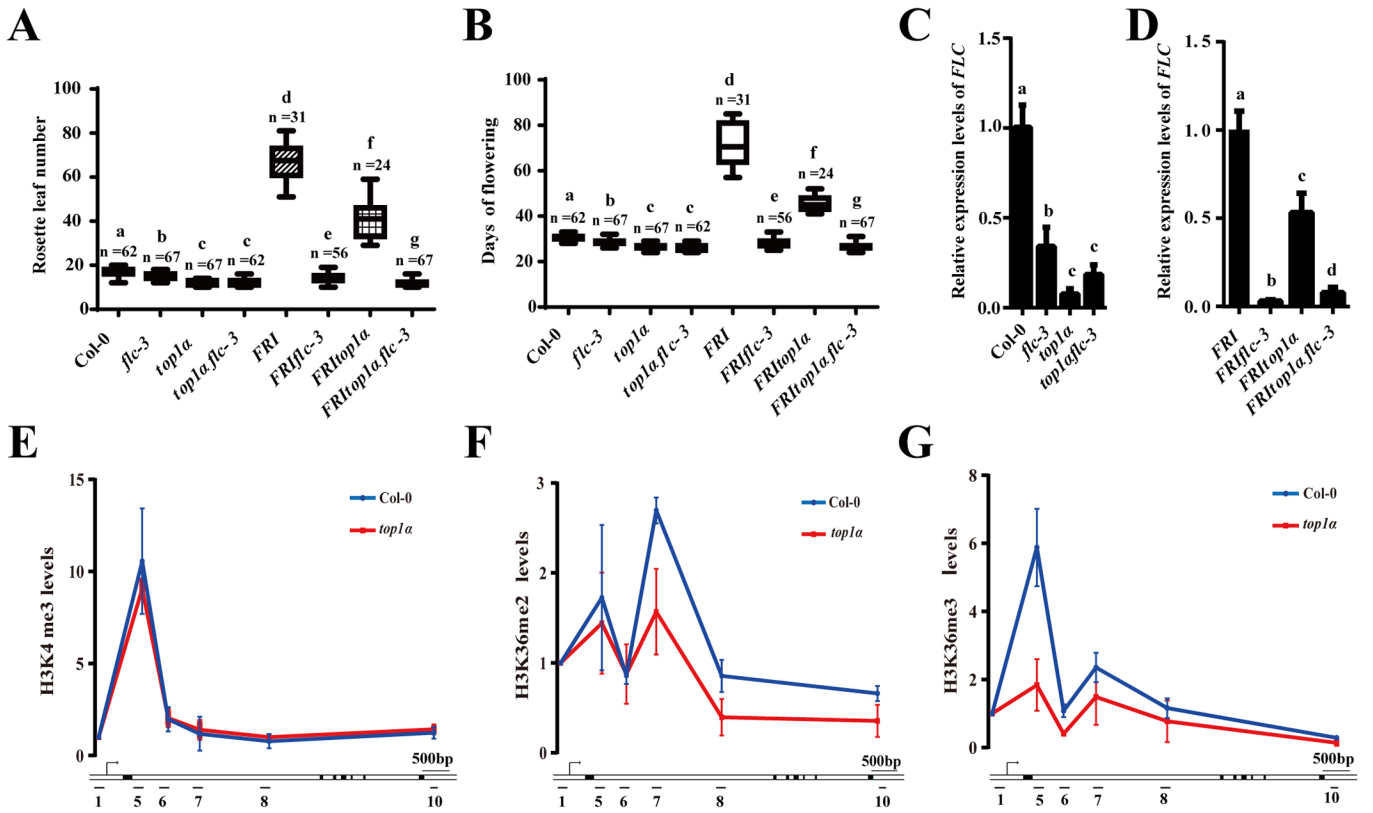

Fig. 1. H3k36me2 and H3k36me3 methylation levels are reduced in the early flowering mutant *top1α*. (A,B) Rosette leaf number (A) and days of flowering (B) of Col-0, *flc-3*, *top1α*, *top1α flc-3*, *FRI*, *FRI flc-3*, *FRI top1α* and *FRI top1α flc-3* under long-day conditions. Mean±s.d. Bars marked with different letters are statistically different to each other (P<0.05 by Student's *t*-test). *n*, the number of plants. (C,D) The relative expression levels of *FLC* were measured by qRT-PCR in Col-0, *flc-3*, *top1α*, *top1α flc-3*, *FRI*, *FRI flc-3*, *FRI top1α* and *FRI top1α flc-3* under long-day conditions. Mean±s.d. of three independent biological replicates. Bars marked with different letters are statistically different to each other (P<0.05 by Student's *t*-test). (E-G) ChIP analysis of H3K4me3 (E), H3K36me2 (F) and H3K36me3 (G) enrichment in the *FLC* locus using 8-day-old Col-0 and *top1α* seedlings. Regions of the *FLC* locus targeted by primer pairs 1, 5, 6, 7, 8 and 10 are shown on the *x*-axis. Exon and untranslated regions are shown as black and white boxes, respectively. Error bars indicate s.d.

Histone modifications, such as H3K4me and H3K36me, are major regulators of chromatin structure at the *FLC* locus and are essential for maintaining high levels of *FLC* transcription (He et al., 2004; Kim et al., 2005; Pien et al., 2008; Shafiq et al., 2014; Tamada et al., 2009; Xu et al., 2008; Zhao et al., 2005). Thus, we further investigated whether *TOP1α*-mediated changes in DNA topological structure affect H3K4 and H3K36 methylations at the *FLC* locus. By performing chromatin immunoprecipitation (ChIP) assays, we observed that H3K4me3 enrichment in the *top1α* mutant was not significantly different compared with that of the wild-type plant at the *FLC* locus (Fig. 1E). However, levels of H3K36me2 and H3K36me3 were dramatically reduced in *top1α* mutants, especially in the 500-1500 bp region downstream of the transcription start sites (TSSs), rather than evenly reduced in the entire gene body (Fig. 1F,G), suggesting that TOP1α is involved in regulating di- and tri-methylation levels of H3K36 at the *FLC* locus in the early phase of transcription elongation.

TOP1α directly interacts with SDG8 in plants

To shed light on the mechanism underlying the ability of TOP1α to regulate H3K36 methylation, we tested whether TOP1α directly recruits SDG8 methyltransferase, which deposits H3K36me2 and H3K36me3 at the *FLC* locus. As the mRNA level of *SDG8* was not affected in the *top1α* mutant (Fig. S4A), we performed yeast two-hybrid assays to examine whether TOP1α (full-length) interacts with the SDG8 fragment from amino acids 335-569 and indeed observed an interaction between TOP1α and SDG8 in yeast cells (Fig. 2A). To test their physical interaction *in vitro*, we performed pull-down assays. Because it is difficult to express the soluble protein of full-length TOP1α in *Escherichia coli* cells, we divided TOP1α into three truncated fragments, TOP1α-1 (amino acids 1-370), TOP1α-2 (370-582) and TOP1α-3 (510-933), and fused the fragments with His-tag (Fig. 2B). We mixed each of these fragments with purified recombinant GST-SDG8 protein *in vitro* and could only detect GST-SDG8 in the presence of His-TOP1α-1 after the His-trapped pull-down, but not in the presence of His-TOP1α-2 or His-TOP1α-3 (Fig. 2C), suggesting that SDG8 directly interacts with the N-terminus of TOP1α. To further confirm the interaction between SDG8 and TOP1α-1 *in vivo*, we performed bimolecular fluorescence complementation (BiFC) experiments in tobacco leaves and observed an interaction between N-terminal enhanced yellow fluorescent protein (eYFP)-fused TOP1α-1 and C-terminal eYFP-fused SDG8 (Fig. 2D). However, the TOP1α-2 fragment did not exhibit any interaction with SDG8 in plants (Fig. 2E). These data suggest that the N-terminus of TOP1α directly interacts with SDG8 in plants.

To test the interaction between TOP1α and SDG8 genetically, we analyzed flowering phenotypes of *top1α*, *sdg8* and *top1α sdg8* mutants. Consistent with previous observations (Gong et al., 2017; Zhao et al., 2005), *top1α* and *sdg8* mutants showed early flowering phenotypes (Fig. 2F,G). We observed the same early flowering phenotypes in *top1α sdg8* mutants based on the total rosette leaf

Development (2019) 146, dev167841. doi:10.1242/dev.167841

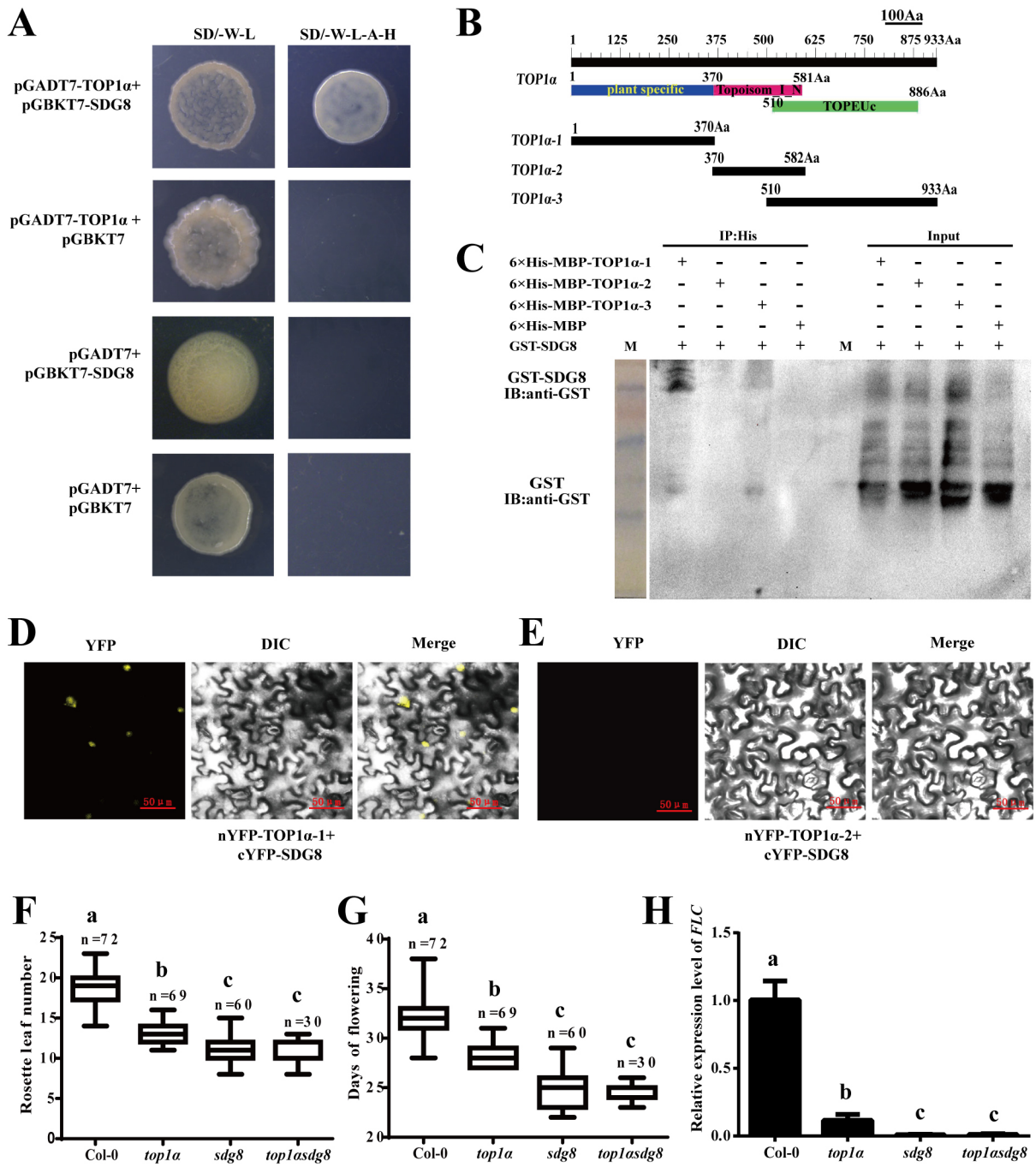

Fig. 2. TOP1α directly interacts with SDG8. (A) Yeast two-hybrid assays were performed to show that full-length TOP1α interacts with the SDG8 fragment consisting of amino acids 335-569. Empty vectors were used as negative controls. SD/-W-L, SD medium lacking Trp and Leu; SD/-W-L-A-H, SD medium lacking Trp, Leu, Ade and His. (B) Schematics showing full-length TOP1α (amino acids 1-933) and three truncated versions, including TOP1α-1 (amino acids 1-370), TOP1α-2 (370-582) and TOP1α-3 (510-933). Aa, amino acid. (C) Pull-down assays showing that SDG8 physically interacts with TOP1α-1 but does not interact with TOP1α-2 or TOP1α-3. M, markers. (D,E) BiFC experiments showed that TOP1α-1 directly interacts with SDG8 in plants (D). TOP1α-2 was used as a negative control (E). DIC, differential interference contrast. Scale bars: 50 µm. (F,G) Rosette leaf numbers (F) and days of flowering (G) in Col-0, *top1α*, *sdg8* and *top1α sdg8* under long-day conditions. Mean±s.d. Bars marked with different letters are statistically different to each other (P<0.05 by Student's *t*-test). *n*, the number of plants. (H) *FLC* expression levels of Col-0, *top1α*, *sdg8* and *top1α sdg8* were measured under long-day conditions. Mean±s.d. of three independent biological replicates. Bars marked with different letters are statistically different to each other (P<0.05 by Student's *t*-test).

number and flowering time (Fig. 2F,G). Moreover, *FLC* expression levels were downregulated in 8-day-old seedlings of *top1α sdg8* mutants, as well as the corresponding single mutants (Fig. 2H), suggesting that *TOP1α* and *SDG8* act in the same genetic pathway to control flowering time.

TOP1α associates with the transcriptional machinery of RNAPII

Early studies in animal cells have demonstrated that TOP1 proteins are deposited at TSSs, where they interact with the phosphorylated carboxyl terminal domain (CTD) of the largest subunit of RNAPII

Development (2019) 146, dev167841. doi:10.1242/dev.167841

to facilitate transcription (Baranello et al., 2016; Carty and Greenleaf, 2002; Kouzine et al., 2013; Teves and Henikoff, 2014; Wu et al., 2010). In *Arabidopsis*, knocking out TOP1α functions causes a significant reduction of RNAPII enrichment at the transcription start site of *FLC* (Gong et al., 2017), whereas the mRNA (Fig. S4B) and protein (Gong et al., 2017) levels are not affected in the *top1α* mutant. To elucidate the molecular mechanism of TOP1α promotion of RNAPII recruitment in plants, we tested whether TOP1α can physically interact with the CTD of RNAPII. By yeast two-hybrid and co-immunoprecipitation (Co-IP) assays, we observed the interaction between CTD and full-length TOP1α in yeast (Fig. 3A) and plant cells (Fig. 3B). As we showed above, SDG8 directly interacted with TOP1α at the N-terminus of TOP1α-1 (Fig. 2C). To explore further the binding fragment of TOP1α with

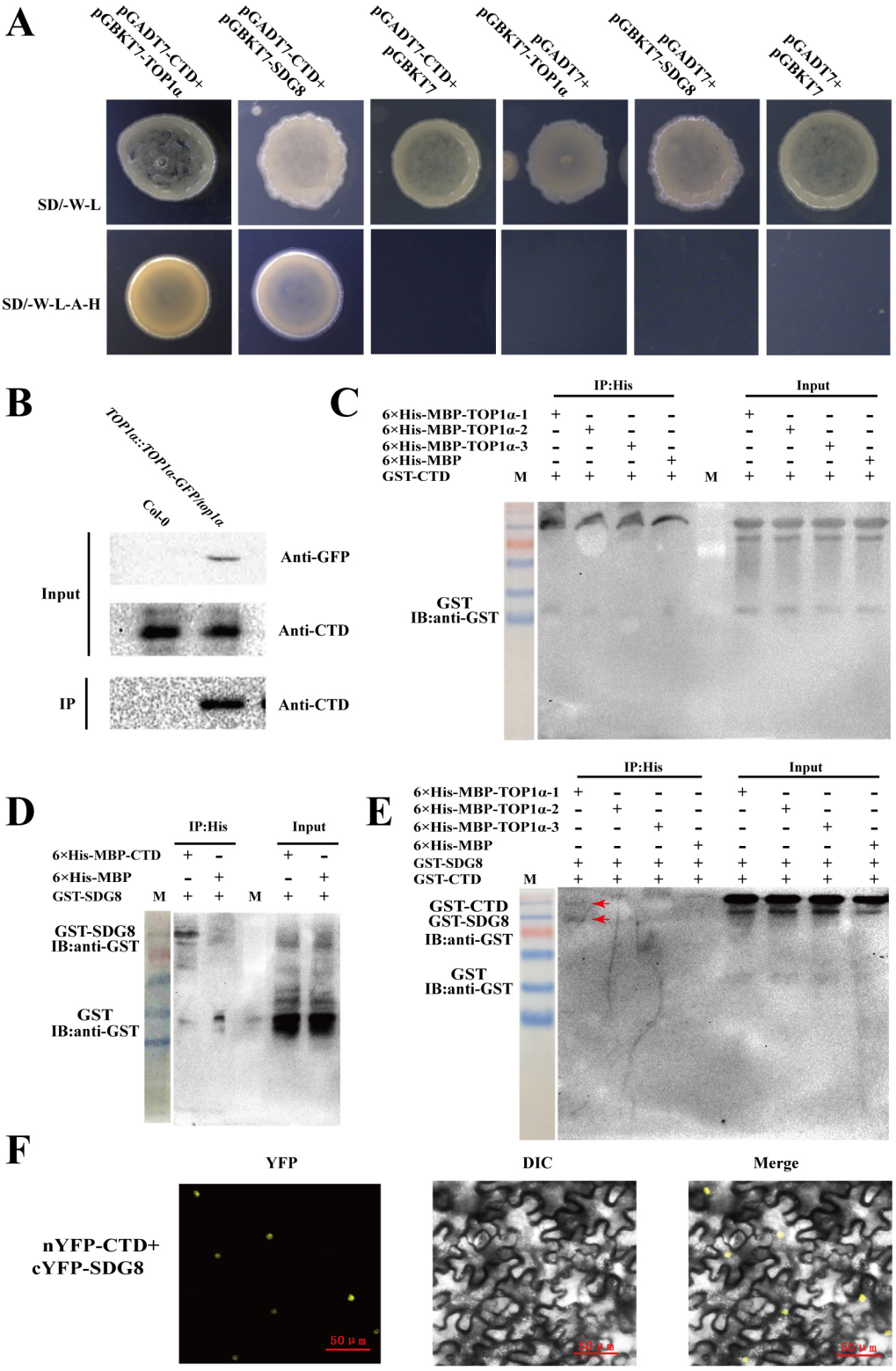

Fig. 3. TOP1α physically associates with the transcriptional machinery. (A) Yeast two-hybrid assays showed that the phosphorylated carboxyl-terminal domain of the largest subunit of RNAPII (CTD) interacts with TOP1α and SDG8. Empty vectors were used as negative controls. SD/-W-L, SD medium lacking Trp and Leu; SD/-W-L-A-H, SD medium lacking Trp, Leu, Ade and His. (B) Co-IP assays showing that TOP1α interacts with the CTD in *Arabidopsis*. (C) Pull-down assays showing that TOP1α does not physically interact with the CTD *in vitro*. (D) Pull-down assays showing that SDG8 physically interacts with the CTD *in vitro*. (E) Pull-down assays showing that TOP1α interacts with CTD in the presence of SDG8. Red arrows indicate two immunoprecipitated bands representing SDG8 and CTD. (F) BiFC experiments showing that CTD directly interacts with SDG8 in tobacco plants. DIC, differential interference contrast; M, markers. Scale bars: 50 μm.

Development (2019) 146, dev167841. doi:10.1242/dev.167841

CTD, the same three truncated forms of TOP1α were used for pull-down assays. We could not detect direct binding of GST-CTD with TOP1α-1, TOP1α-2 or TOP1α-3 (Fig. 3C).

Given that TOP1α directly bonds with SDG8, we then investigated whether TOP1α could recruit RNAPII via SDG8 to form a complex. To this end, we first confirmed the direct interaction between CTD and SDG8 by using yeast two-hybrid (Fig. 3A), pull-down (Fig. 3D) and BiFC assays (Fig. 3F). Then we performed TOP1α pull-down assays with GST-CTD in the presence of GST-SDG8, and observed two immunoprecipitated bands representing SDG8 and CTD (Fig. 3E), suggesting that TOP1α interacts with RNAPII indirectly via SDG8. We further performed BiFC-based fluorescence resonance energy transfer (FRET) to examine the interaction of three proteins at the same time in plants. We co-transformed *35S::CFP-TOP1α-1*, *35S::nYFP-CTD* and *35S::cYFP-SDG8* into tobacco leaves, and observed energy transfer from CFP to YFP (Fig. S5), suggesting that TOP1α, CTD and SDG8 are in the same complex.

TOP1α regulates early transcription elongation by recruiting RNAPII and H3K36 methyltransferase

RNAPII enrichment in the *top1α* mutant was found to be significantly reduced, including at the first intron where the major regulatory region for epigenetic modifications is located (Ausín et al., 2004; Bastow et al., 2004; He et al., 2004, 2003; Sheldon et al., 2002; Sung and Amasino, 2004), indicating a role for TOP1α in transcription beyond its recruitment of RNAPII, although it is unknown if and how TOP1α activity is involved in the transcription elongation of *FLC*. To test this hypothesis functionally, we measured the transcriptional levels of *FLC* across the entire locus by designing a series of primers from the TSS to the last exon. We observed, surprisingly, that in the *top1α* mutant, transcripts of *FLC* were not reduced evenly across the entire locus but rather a dramatic decrease of over 80% at the beginning of transcription elongation, 300-500 bp downstream from the TSS, was observed with relatively stable expression levels thereafter (Fig. 4A). This non-uniform transcription pattern of *FLC* in the *top1α* mutant strongly suggests that TOP1α participates in the early phase of transcription elongation. As TOP1α directly interacts with SDG8, which deposited H3K36 methylation in the *FLC*, we then asked whether downregulation of H3K36 methylation might also cause the same reduction of *FLC* at the early stages of elongation. In the *sdg8* mutant, we observed very similar transcription patterns along the *FLC* locus, with transcripts decreasing by 90% in the same region as observed for *top1α* (Fig. 4B), demonstrating that H3K36 methylation is functionally linked with early transcription elongations. Consistent with this observation, we found a major enrichment peak of H3K36me3 in the *FLC* locus, which was located at the beginning of the first intron (region 5, approximately 500 bp away from the TSS) (Fig. 4C). The di-methylated forms of H3K36 were mainly deposited in the middle of the first intron 1500 bp away from the TSS (Fig. 4D). In the *top1α* mutant, the H3K36me3 deposition in *FLC* was mainly reduced in the region of its highly enriched peak (Fig. 1G). From the TSS to this region we observed a rapid decrease of *FLC* transcripts in *top1α* (Fig. 4A) and *sdg8* (Fig. 4B) mutants. Given that TOP1α interacts with SDG8 and CTD, we conclude that TOP1α regulates early phases of

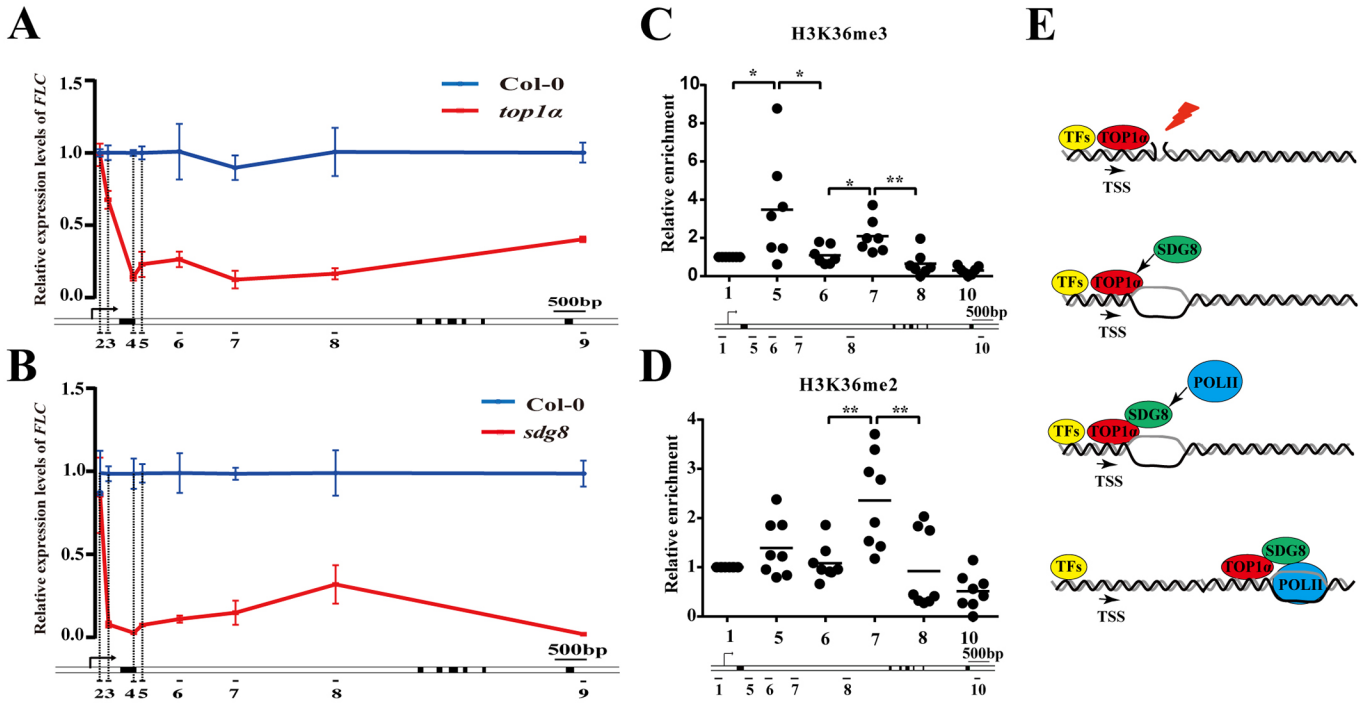

Fig. 4. TOP1α facilitates transcriptional elongation by recruiting H3K36 methyltransferase. (A,B) The relative expression levels of *FLC* among different regions, which were measured by qRT-PCR using a series of primers (2-9) across the entire locus. In *top1α* (A) and *sdg8* (B) 8-day-old seedlings, *FLC* transcripts decreased dramatically at the beginning of transcription elongation, which was downstream of the TSS. All experiments were performed with three independent biological replicates. Mean±s.d. (C,D) ChIP analysis of H3K36me2 (D) and H3K36me3 (C) enrichment in the wild-type *FLC* locus using 8-day-old seedlings. **P*<0.05, ***P*<0.01 by Student's *t*-test. Each black dot represents an independent experiment. Regions of the *FLC* locus targeted by primer pairs 1-10 are shown on the *x*-axis. The black arrow shows the TSS, which was located –269 bp upstream of ATG (+1). Exon and untranslated regions are shown as black and white boxes, respectively. (E) Hypothetical regulatory mechanism of TOP1α-mediated transcription elongation in *FLC*. TOP1α directly binds the TSS to relax unfavorable DNA supercoils by the transient cleavage of DNA, interacts with H3K36me3 methyltransferases to establish a permissive histone modification and recruits the RNA polymerase (POLII) to facilitate the transcription elongation of *FLC*. TFs, transcription factors.

Development (2019) 146, dev167841. doi:10.1242/dev.167841

transcription elongation in *FLC* by recruiting H3K36 methyltransferase and RNAPII.

The early phases of transcription are coupled with recruitment of the transcription initiation complex and movement of the transcription machinery along the gene bodies. Our data are not consistent with the observation in animals that TOP1α directly interacts with RNAPII to form the transcription complex. In contrast, in plants TOP1α recruits RNAPII via SDG8 to promote early transcription elongation by maintaining the open chromatin state via H3K36 methylation (Fig. 4E), suggesting that TOP1α-mediated topological relaxation of the DNA template and recruitment of permissive histone modifications are essential for the early transcription elongation of *FLC*.

TOP1 in animals has been reported to interact with RNAPII to regulate transcription pauses (Baranello et al., 2016). We found that TOP1α in plants interacts with SDG8 to recruit RNAPII at the N-terminus. The N-terminal domain of TOP1α is a plant-specific fragment that is not conserved in animals (Fig. S6), and its function is not known. Our data indicate that the recruitment of histone modifications to regulate transcription might be a unique feature of plant type IB topoisomerases. Interestingly, in plants, TOP1α is also required for silencing Polycomb group (PcG) target genes by increasing the repressive mark of H3K27me3 at the promoter region (Liu et al., 2014), or transposable elements by RNAPV-dependent RNA-directed DNA methylation (RdDM) and H3K9me2 (Dinh et al., 2014). Therefore, it remains to be determined whether TOP1α directly recruits a variety of histone methyltransferases and different types of RNA polymerases to either positively or negatively regulate gene expression at different transcriptional stages, and how these activities are specified during plant development.

MATERIALS AND METHODS

Plant materials and growth conditions

All plants were in the Columbia-0 (Col-0) background except for *FRI* (CS6209), which was obtained from *Arabidopsis* Biological Resource Center (ABRC). The *top1α* mutant (*top1α-1*) was kindly provided by Prof. Taku Takahashi (Okayama University, Japan). The *sdg8* mutant (SALK_036941) and *flc-3* were kindly provided by Prof. Yong Ding (University of Science and Technology of China, China). The *FRIflc-3* mutant was kindly provided by Prof. Ya-Long Guo (Institute of Botany, Chinese Academy of Sciences, China). All mutants of *FRItop1α*, *FRItop1αflc-3*, *top1αsdg8* and *top1αflc-3* were obtained by crossing the above mutants. All seeds were sterilized by applying 70% ethanol and 0.5% Tween 20 for 10 min, followed by two washes with 95% ethanol and air drying. Plants were grown at 21°C under long-day conditions (16 h of light and 8 h of darkness). All materials for quantitative RT-PCR and ChIP-PCR were 8-day-old seedlings grown on 1/2 Murashige and Skoog (MS) medium containing 0.8% agar and 0.5% sucrose under long-day conditions.

Total RNA isolation and quantitative RT-PCR

Seedlings were collected and immediately transferred to liquid nitrogen. The Tripure Isolation Reagent (Roche, 94002420) was used to isolate total RNA from plant samples. The PrimeScript RT Reagent Kit (TaKaRa, RR047A) was used for cDNA synthesis. Primers used for qRT-PCR were designed to amplify products that were 100-300 bp in length; gene-specific primer sequences are listed in Table S1. Quantitative PCR was performed with the Thermo PIKO REAL96 Real-Time PCR system using the GoTaq qPCR Master Mix (Promega) with the following conditions: 95°C for 5 min; 40 cycles of 95°C for 10 s, 57°C for 30 s and 72°C for 30 s, followed by 72°C for 10 min. *TUBULIN* was used to normalize mRNA levels.

The primer pairs used for quantitative RT-PCR (Fig. 4A,B) were: 2, −269 bp upstream of ATG; 3, −200 bp upstream of ATG; 4, 71 bp downstream of ATG; 5, 201 bp downstream of ATG; 6, 688 bp downstream of ATG; 7, 1306 bp downstream of ATG; 8, 2562 bp downstream of ATG; 9, 5506 bp downstream of ATG.

Chromatin immunoprecipitation

Chromatin immunoprecipitation (ChIP) experiments were performed as previously described (Leibfried et al., 2005). Total chromatin was extracted from 8-day-old seedlings and the Diagenode Bioruptor UCD-200 was used for sonication (30 s on, 30 s off, medium, 40 min duration; sonication buffer: 10 mM Na_3PO_4, 100 mM NaCl, 0.5% sarkosyl, 10 mM EDTA, 1 mM PMSF, protease inhibitor, 1 tablet per 10 ml, pH 7). Chromatin was immunoprecipitated with anti-GFP (Abcam, ab290), anti-H3K4me3 (Abcam, ab8050), anti-H3K36me2 (Abcam, ab9049), anti-H3K36me3 (Abcam, ab9050) and anti-CTD (Abcam, ab1791) antibodies used at 1:200. Quantitative real-time PCR was conducted to measure the amounts of immunoprecipitated fragments of genes of interest on the Thermo PIKO REAL96 Real-Time PCR system using a GoTaq qPCR Master Mix (Promega), and each ChIP sample was quantified in triplicate. The primer pairs used for ChIP-qPCR in Fig. 1E,F and Fig. 4C,D were: 1, −662 bp upstream of ATG (+1); 5, 201 bp downstream of ATG; 6, 688 bp downstream of ATG; 7, 1306 bp downstream of ATG; 8, 2562 bp downstream of ATG; and 10, 5730 bp downstream of ATG. The TSS was located −269 bp upstream of ATG (+1). The primer sequences used for ChIP are listed in Table S1.

Yeast two-hybrid assay

The yeast two-hybrid assay was performed according to the standard protocol of Clontech (Clontech, user manual 630489). *Saccharomyces cerevisiae* strain AH109 was co-transformed with the bait and prey constructs of *pGBKT7-SDG8* (amino acids 335-569) and *pGADT7-TOP1α* (full length); *pGBKT7-TOP1α* (full length) and *pGADT7-CTD*; and *pGBKT7-SDG8* and *pGADT7-TOP1α*. Vectors without coding region insertions were used as negative controls. The growth of yeast cells on synthetic defined (SD) medium lacking Trp, Leu, His and adenine was used to detect the interaction.

Protein pull-down assays

Total protein was purified from *E. coil* (*Rosetta*) that were transformed by the following constructs: *6×His-MBP-TOP1α-1* (from amino acids 1-370), *6×His-MBP-TOP1α-2* (370-582), *6×His-MBP-TOP1α-3* (510-933), *6×His-MBP-CTD*, *GST-SDG8* (335-569) and *GST-CTD*.

Glutathione-Sepharose beads (GE Healthcare; Lot: 10236606) were used for the purification of GST-tagged proteins by washing solution [50 mM Tris-HCl, 200 mM NaCl, 1 mM reduced glutathione, 0.2% (v/v) Triton X-100, pH 8.0] and elution solution (50 mM Tris-HCl, 150 mM NaCl, 20 mM reduced glutathione, pH 8.0). Ni-Sepharose beads (GE Healthcare; Lot: 10233021) were used for the purification of His-tagged proteins by washing solution (50 mM Tris-HCl, 200 mM NaCl, 10 mM imidazole, pH 8.0) and elution solution (50 mM Tris-HCl, 150 mM NaCl, 250 mM imidazole, pH 8.0).

Beads were incubated with bait proteins at 4°C for 1 h with 5% skim milk powder in the pull-down solution (20 mM Tris-HCl pH 8.0, 200 mM NaCl, 1 mM EDTA pH 8.0, 0.25% NP-40 and 25 ng/µl PMSF) and then beads were washed several times with the same pull-down solution. Beads were then incubated with 5 µg of soluble protein in 600 µl pull-down solution for 3 h at 4°C. Mock controls included extracts prepared from either the His-Tag or GST-tag vectors. The supernatant was collected as input. The beads were washed five to eight times with pull-down solution, separated on an SDS-PAGE gel, and detected by anti-GST antibody (GenScript, A00866-100, Lot: 13D000626).

Co-immunoprecipitation (Co-IP)

Eight-day-old seedlings of Col-0 and *pTOP1α:: TOP1α-GFP*/*top1α* were used for Co-IP assays. One gram of seedlings was harvested and ground in liquid nitrogen, mixed with 2 ml protein extraction buffer containing 50 mM Tris-HCl, pH 7.4, 150 mM NaCl, 1 mM EDTA, 0.1% (v/v) Triton X-100, 10% (v/v) glycerin, 1 mM PMSF (added fresh) and 1 mM Protease Inhibitor Cocktail (Okayama University, Japan; added fresh). After 3 h on ice and centrifugation at 12,000 ***g***, 100 µl supernatant (total protein) was used as the input, and 30 µl protein A beads (Invitrogen, 1002D) were added to the total protein and incubated on ice for 1 h. To detect protein interactions, 2 µg anti-GFP antibody (Abcam, ab290) was added to the supernatant and incubated overnight. After adding 50 µl protein A beads and incubating for 3 h, beads

Development (2019) 146, dev167841. doi:10.1242/dev.167841

were washed three times with protein extraction buffer before being separated by SDS-PAGE, and analyzed by western blot using an anti-CTD antibody (Abcam, ab1791 1:1000).

Bimolecular fluorescence complementation (BiFC)

Nicotiana benthamiana were grown in growth chambers under long-day conditions at 21°C. *Agrobacterium* was transformed with relevant binary vectors of *35S::nYFP-TOP1α-1*, *35S::nYFP-TOP1α-2*, *35S::nYFP-CTD*, *35S::cYFP-CTD* and *35S::cYFP-SDG8*. A 1:1 mixture of two different bacteria containing plasmids of interest was used to infiltrate the abaxial leaves of 3- to 4-week-old *N. benthamiana*. Epidermal cells of *N. benthamiana* were examined 48-72 h after infiltration with a spectral confocal laser-scanning microscope (Leica, LSM710).

BiFC-based FRET assays

Agrobacterium was transformed with relevant binary vectors of *35S::CFP-TOP1α-1*, *35S::nYFP-CTD* and *35S::cYFP-SDG8*. A 1:1:1 mixture of three different bacteria containing plasmids of interest was used to infiltrate the abaxial leaves of 3- to 4-week-old *N. benthamiana*. Epidermal cells of *N. benthamiana* were examined 72 h after infiltration with a spectral confocal laser-scanning microscope (Leica, LSM710). The excitation wavelength used to excite the donor molecule (CFP) was 448 nm from an argon ion laser, and 514 nm was used to acquire the acceptor (YFP) image.

Complementation

The *pTOP1α:: TOP1α-GFP* was used to transform *top1α* mutants by the floral-dip method (Clough and Bent, 1998). Those rescued transgenic plants that carried a single insertion in the genome were used for further analysis.

In situ hybridization

The template of *TOP1α* was amplified by PCR with specific primers containing T7 and T3 promoter sequences. RNA probes were synthesized by T7/T3 polymerase and labeled with digoxin-UTP. Then, *in situ* hybridization was performed according to standard protocols (Andersen et al., 2008; Weigel and Jürgens, 2002).

Microscopy

Eight-day-old seedlings of *pTOP1α:: TOP1α-GFP/top1α* rescue plants were embedded in 6% low melting agarose (Promega, V2111), and sectioned with a vibratome (Leica, VT 1200S) at 100 µm thickness. The sections were collected and immediately imaged with a confocal microscope (Leica, LSM710).

Acknowledgements

We thank Prof. Taku Takahashi, Prof. Yong Ding and Prof. Ya-Long Guo for sharing mutant seeds.

Competing interests

The authors declare no competing or financial interests.

Author contributions

Conceptualization: Z.Z., Z.T.; Methodology: P.Z., J.L., L.L.; Validation: P.Z., J.L.; Formal analysis: P.Z., J.L., L.L., Z.Z., Z.T.; Investigation: P.Z., J.L., L.L., Z.T.; Resources: P.Z.; Data curation: P.Z.; Writing - original draft: P.Z., Z.Z., Z.T.; Writing - review & editing: Z.Z., Z.T.; Supervision: Z.Z., Z.T.; Project administration: Z.Z., Z.T.; Funding acquisition: Z.Z., Z.T.

Funding

This work was supported by the National Natural Science Foundation of China (31300248 to Z.T., 31570273 to Z.Z.).

Supplementary information

Supplementary information available online at
http://dev.biologists.org/lookup/doi/10.1242/dev.167841.supplemental

References

Andersen, S. U., Buechel, S., Zhao, Z., Ljung, K., Novak, O., Busch, W., Schuster, C. and Lohmann, J. U. (2008). Requirement of B2-type cyclin-dependent kinases for meristem integrity in Arabidopsis thaliana. *Plant Cell* **20**, 88-100.

Ausín, I., Alonso-Blanco, C., Jarillo, J. A., Ruiz-García, L. and Martínez-Zapater, J. M. (2004). Regulation of flowering time by FVE, a retinoblastoma-associated protein. *Nat. Genet.* **36**, 162-166.

Baranello, L., Wojtowicz, D., Cui, K., Devaiah, B. N., Chung, H.-J., Chan-Salis, K. Y., Guha, R., Wilson, K., Zhang, X., Zhang, H. et al. (2016). RNA polymerase II regulates topoisomerase 1 activity to favor efficient transcription. *Cell* **165**, 357-371.

Bastow, R., Mylne, J. S., Lister, C., Lippman, Z., Martienssen, R. A. and Dean, C. (2004). Vernalization requires epigenetic silencing of FLC by histone methylation. *Nature* **427**, 164-167.

Carty, S. M. and Greenleaf, A. L. (2002). Hyperphosphorylated C-terminal repeat domain-associating proteins in the nuclear proteome link transcription to DNA/chromatin modification and RNA processing. *Mol. Cell. Proteomics* **1**, 598-610.

Champoux, J. J. (2001). DNA topoisomerases: structure, function, and mechanism. *Annu. Rev. Biochem.* **70**, 369-413.

Clough, S. J. and Bent, A. F. (1998). Floral dip: a simplified method for Agrobacterium-mediated transformation of Arabidopsis thaliana. *Plant J.* **16**, 735-743.

Dinh, T. T., Gao, L., Liu, X., Li, D., Li, S., Zhao, Y., O'Leary, M., Le, B., Schmitz, R. J., Manavella, P. et al. (2014). DNA topoisomerase 1α promotes transcriptional silencing of transposable elements through DNA methylation and histone lysine 9 dimethylation in Arabidopsis. *PLoS Genet.* **10**, e1004446.

Gong, X., Shen, L., Peng, Y. Z., Gan, Y. and Yu, H. (2017). DNA topoisomerase Ialpha affects the floral transition. *Plant Physiol.* **173**, 642-654.

Graf, P., Dolzblasz, A., Wurschum, T., Lenhard, M., Pfreundt, U. and Laux, T. (2010). MGOUN1 encodes an Arabidopsis type IB DNA topoisomerase required in stem cell regulation and to maintain developmentally regulated gene silencing. *Plant Cell* **22**, 716-728.

He, Y., Michaels, S. D. and Amasino, R. M. (2003). Regulation of flowering time by histone acetylation in Arabidopsis. *Science* **302**, 1751-1754.

He, Y., Doyle, M. R. and Amasino, R. M. (2004). PAF1-complex-mediated histone methylation of FLOWERING LOCUS C chromatin is required for the vernalization-responsive, winter-annual habit in Arabidopsis. *Genes Dev.* **18**, 2774-2784.

Johanson, U., West, J., Lister, C., Michaels, S., Amasino, R. and Dean, C. (2000). Molecular analysis of FRIGIDA, a major determinant of natural variation in Arabidopsis flowering time. *Science* **290**, 344-347.

Kieber, J. J., Tissier, A. F. and Signer, E. R. (1992). Cloning and characterization of an Arabidopsis thaliana topoisomerase I gene. *Plant Physiol.* **99**, 1493-1501.

Kim, S. Y., He, Y., Jacob, Y., Noh, Y. S., Michaels, S. and Amasino, R. (2005). Establishment of the vernalization-responsive, winter-annual habit in Arabidopsis requires a putative histone H3 methyl transferase. *Plant Cell* **17**, 3301-3310.

Kouzine, F., Gupta, A., Baranello, L., Wojtowicz, D., Ben-Aissa, K., Liu, J., Przytycka, T. M. and Levens, D. (2013). Transcription-dependent dynamic supercoiling is a short-range genomic force. *Nat. Struct. Mol. Biol.* **20**, 396-403.

Laufs, P., Dockx, J., Kronenberger, J. and Traas, J. (1998). MGOUN1 and MGOUN2: two genes required for primordium initiation at the shoot apical and floral meristems in Arabidopsis thaliana. *Development* **125**, 1253-1260.

Leibfried, A., To, J. P., Busch, W., Stehling, S., Kehle, A., Demar, M., Kieber, J. and Lohmann, J. U. (2005). WUSCHEL controls meristem function by direct regulation of cytokinin-inducible response regulators. *Nature* **438**, 1172-1175.

Liu, X., Gao, L., Dinh, T. T., Shi, T., Li, D., Wang, R., Guo, L., Xiao, L. and Chen, X. (2014). DNA topoisomerase I affects polycomb group protein-mediated epigenetic regulation and plant development by altering nucleosome distribution in Arabidopsis. *Plant Cell* **26**, 2803-2817.

Michaels, S. D. and Amasino, R. M. (1999). FLOWERING LOCUS C encodes a novel MADS domain protein that acts as a repressor of flowering. *Plant Cell* **11**, 949-956.

Michaels, S. D. and Amasino, R. M. (2001). Loss of FLOWERING LOCUS C activity eliminates the late-flowering phenotype of FRIGIDA and autonomous pathway mutations but not responsiveness to vernalization. *Plant Cell* **13**, 935-942.

Pien, S., Fleury, D., Mylne, J. S., Crevillen, P., Inze, D., Avramova, Z., Dean, C. and Grossniklaus, U. (2008). ARABIDOPSIS TRITHORAX1 dynamically regulates FLOWERING LOCUS C activation via histone 3 lysine 4 trimethylation. *Plant Cell* **20**, 580-588.

Shafiq, S., Berr, A. and Shen, W.-H. (2014). Combinatorial functions of diverse histone methylations in Arabidopsis thaliana flowering time regulation. *New Phytol.* **201**, 312-322.

Sheldon, C. C., Conn, A. B., Dennis, E. S. and Peacock, W. J. (2002). Different regulatory regions are required for the vernalization-induced repression of FLOWERING LOCUS C and for the epigenetic maintenance of repression. *Plant Cell* **14**, 2527-2537.

Sung, S. and Amasino, R. M. (2004). Vernalization in Arabidopsis thaliana is mediated by the PHD finger protein VIN3. *Nature* **427**, 159-164.

Takahashi, T., Matsuhara, S., Abe, M. and Komeda, Y. (2002). Disruption of a DNA topoisomerase I gene affects morphogenesis in Arabidopsis. *Plant Cell* **14**, 2085-2093.

Tamada, Y., Yun, J.-Y., Woo, S. C. and Amasino, R. M. (2009). ARABIDOPSIS TRITHORAX-RELATED7 is required for methylation of lysine 4 of histone H3 and for transcriptional activation of FLOWERING LOCUS C. *Plant Cell* **21**, 3257-3269.

Development (2019) 146, dev167841. doi:10.1242/dev.167841

Teves, S. S. and Henikoff, S. (2014). Transcription-generated torsional stress destabilizes nucleosomes. *Nat. Struct. Mol. Biol.* **21**, 88-94.

Weigel, D. and Jürgens, G. (2002). Stem cells that make stems. *Nature* **415**, 751-754.

Wu, J., Phatnani, H. P., Hsieh, T. S. and Greenleaf, A. L. (2010). The phosphoCTD-interacting domain of Topoisomerase I. *Biochem. Biophys. Res. Commun.* **397**, 117-119.

Xu, L., Zhao, Z., Dong, A., Soubigou-Taconnat, L., Renou, J.-P., Steinmetz, A. and Shen, W.-H. (2008). Di- and tri- but not monomethylation on histone H3 lysine 36 marks active transcription of genes involved in flowering time regulation and other processes in Arabidopsis thaliana. *Mol. Cell. Biol.* **28**, 1348-1360.

Zhao, Z., Yu, Y., Meyer, D., Wu, C. and Shen, W.-H. (2005). Prevention of early flowering by expression of FLOWERING LOCUS C requires methylation of histone H3 K36. *Nat. Cell Biol.* **7**, 1256-1260.